catalysts

MDPI

Article

Carbon-Modified Mesoporous Anatase/TiO_2(B) Whisker for Enhanced Activity in Direct Synthesis of Hydrogen Peroxide by Palladium

Rui Tu [1], Licheng Li [2], Suoying Zhang [1], Shuying Chen [1], Jun Li [1,*] and Xiaohua Lu [1,*]

[1] State Key Laboratory of Materials-Oriented Chemical Engineering, College of Chemical Engineering, Nanjing Tech University, Nanjing 210009, China; ruitu@njtech.edu.cn (R.T.); iamsyzhang@njtech.edu.cn (S.Z.); csy1002@njtech.edu.cn (S.C.)

[2] College of Chemical Engineering, Nanjing Forestry University, Nanjing 210037, China; llc0024@yahoo.com

* Correspondence: lijun@njtech.edu.cn (J.L.); xhlu@njtech.edu.cn (X.L.); Tel.: +86-25-8358-8063 (X.L.)

Academic Editor: Morris D. Argyle

Received: 16 March 2017; Accepted: 22 May 2017; Published: 2 June 2017

Abstract: The regulation of the interaction between H_2O_2 and its catalysts is a promising route to achieve high productivity and selectivity towards H_2O_2. Herein, mesoporous anatase/TiO_2(B) whisker (mb-TiO_2) modified with heterogeneous carbon was prepared as the support of Pd-based catalysts for the direct synthesis of H_2O_2. The morphology and structure of the catalyst were investigated by transmission electron microscopy, X-ray diffraction, Raman spectroscopy, Brunner-Emmet-Teller measurements, and X-ray photoelectron spectroscopy. The interaction between H_2O_2 and the support was studied by isothermal calorimeter. The carbon heterogeneous modification can weaken the interaction between H_2O_2 and the support, then accelerate the desorption of H_2O_2 and reduce the re-adsorption of H_2O_2 in the reaction medium. Meanwhile, the synergistic effects between TiO_2 and Pd nanoparticles are not influenced by the heterogeneous carbon distribution. The catalyst exhibits better performance for the synthesis of H_2O_2 compared with the corresponding unmodified catalyst; the productivity of H_2O_2 increases more than 40%, which can be ascribed to the decrease of further H_2O_2 conversion under the weakened interaction.

Keywords: direct synthesis of H_2O_2; mesoporous anatase/TiO_2(B) whisker; carbon modification; palladium; H_2O_2 desorption; isothermal microcalorimetry

1. Introduction

As a green and excellent oxidant, hydrogen peroxide (H_2O_2) has been widely applied in the pulp/paper industry, water purification, and chemical synthesis [1]. With the increasing demand for H_2O_2 in the international market, the direct synthesis of H_2O_2 from hydrogen and oxygen is believed to be a promising route because of its remarkable advantages [2–7], such as its lower levels of environmental pollution and lower cost. However, three inevitable side reactions in the direct synthesis process, including the combustion of H_2 and the hydrogenation/decomposition of H_2O_2, reduce the productivity and selectivity towards H_2O_2, which is the major drawback of this process [2,4,8].

The surface property of the support has been proved to have an important effect on the performance of H_2O_2 synthesis. For example, the hydrophilic/hydrophobic moderation of the support is an efficient approach to improve the catalytic activity. As early as the 1970s, Pd catalysts supported on more hydrophobic materials were prepared to improve the productivity of H_2O_2 [9]. Hu et al. came to similar conclusions; they speculated further that more hydrophilic support might increase the re-adsorption of H_2O_2, resulting in the further conversion of H_2O_2 and the lower selectivity of H_2O_2 synthesis [8]. In addition, the crystal phase of the support surface can also lead to the enhancement of

catalytic performance by the suppression of side reactions. TiO_2 is a promising candidate support for H_2O_2 synthesis and has been widely studied [10–12]. According to our previous work with assistance from molecular dynamic simulations [13], it has been indicated that introducing the proper amount of TiO_2(B) phase in the catalyst surface can accelerate the desorption of H_2O_2 from the catalyst due to the weak interaction between H_2O_2 and TiO_2(B), and consequently improve the productivity of H_2O_2 over Pd-TiO_2(B)/anatase catalyst.

In fact, the interaction between H_2O_2 and the support is the origin of the support effect according to the analysis mentioned above, and the selectivity and productivity of H_2O_2 is thus influenced by the moderation of the interaction between H_2O_2 and the support. Carbon-modified TiO_2 has been proved to weaken the adsorption of polar molecules and accelerate their transfer [14]. Meanwhile, the carbon modification method is facile, inexpensive, and minimally changes the structure of supports. Herein, we fabricated a heterogeneous carbon-modified catalyst for the direct synthesis of H_2O_2 on the basis of mesoporous anatase/TiO_2(B) whisker (mb-TiO_2). mb-TiO_2 whisker with excellent performance in various catalytic systems has been successfully prepared in our previous work [15–18]. Carbon heterogeneous surface modification can regulate the adsorption of H_2O_2 on the catalyst surface without changing the strong synergy between active sites and TiO_2. The experimental results showed that the Pd-supported, carbon-modified mb-TiO_2 (C-mb-TiO_2) catalyst exhibited higher productivity and selectivity towards H_2O_2 compared with the unmodified Pd/mb-TiO_2 catalyst. X-ray diffraction (XRD), Raman spectra, transmission electron microscopy (TEM), X-ray photoelectron spectroscopy (XPS), and isothermal microcalorimeter (IMC) characterization techniques were applied to analyze the structure–performance relationship.

2. Results and Discussion

2.1. Structural Characterization of the Catalysts

Figure 1 shows the XRD and Raman patterns of mb-TiO_2, C-mb-TiO_2, and the corresponding Pd-supported catalysts. Five distinct diffraction peaks are assigned to anatase phase of TiO_2 (JCPDF 21-1272) [19]. Meanwhile, the weak observed peaks at 2θ of 14.3°, 28.7° and 43.6° correspond to (001), (002) and (003) of TiO_2(B) phase (JCPDF 35-0088) [20]. Evidently, no extra diffraction peaks of carbon can be found in C-mb-TiO_2, which implies that either the amount of carbon is too little or the generated carbon is amorphous [21]. In addition, the diffraction peaks for Pd are indistinguishable, which may be caused by the low content or good dispersion, as previously reported [22]. The bicrystalline structure was also confirmed by Raman spectra. Peaks at 234 cm^{-1}, 431 cm^{-1} and 469 cm^{-1} are all indexed to the TiO_2(B) phase [13]. The specific crystal structure has been explored in our previous work [15]. As shown in Figure 1b, two Raman bands located at 1300–1450 cm^{-1} (D-band) and 1500–1650 cm^{-1} (G-band) are only observed in C-mb-TiO_2 rather than mb-TiO_2, which verifies the existence of carbon species on the surface of C-mb-TiO_2 [8]. The TG analysis shows that the content of carbon species of C-mb-TiO_2 is less than 1 wt % (seen in Figure S2), and only about one third of mb-TiO_2 surface is covered by the introduced carbon species according to our previous calculation [14].

N_2 adsorption-desorption isotherms were measured at 77 K to characterize the physical and chemical properties of supports and corresponding catalysts, as shown in Figure 2. The typical type IV isotherms according to IUPAC classification are observed for all samples, indicating the presence of a mesoporous structure [17]. The corresponding pore size distribution curves (seen in Figure 2) show a narrow distribution ranging from 5 to 9 nm with a maximum around 7 nm for all samples. Details about the BET surface area and average pore volume/size are summarized in Table 1. It can be seen that the surface area and pore volume of C-mb-TiO_2 are nearly identical to that of mb-TiO_2, indicating that almost nothing has changed in the initial structure of mb-TiO_2 after the carbon modification. Both the average pore size and the pore volume decrease after loading with Pd, which can be ascribed to the adhesion of metallic Pd nanoparticles inside the pores.

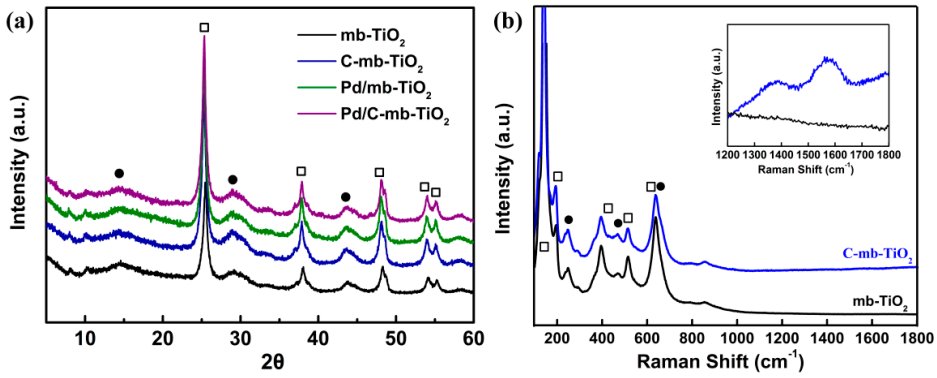

Figure 1. (**a**) XRD pattern and (**b**) Raman spectra of the samples. (□ anatase, ● TiO_2(B)).

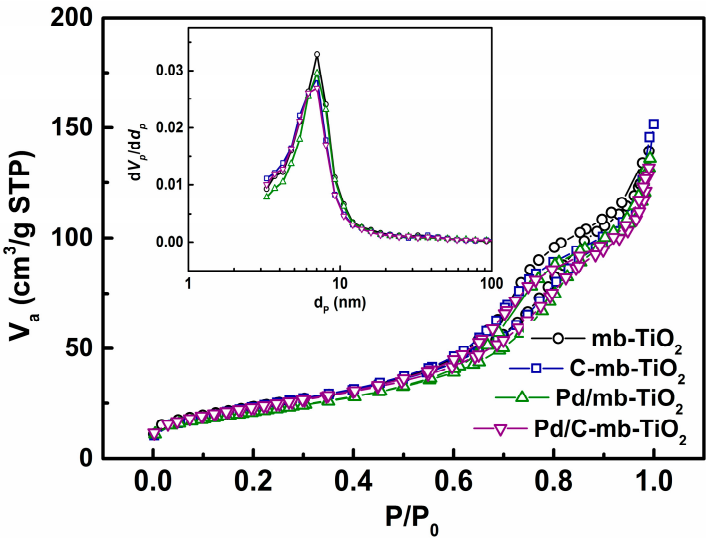

Figure 2. N_2 adsorption-desorption isotherms and the pore-size distribution of the samples.

Table 1. Structural properties of the supports and catalysts.

Sample	Surface Area ($m^2 \cdot g^{-1}$)	Pore Volume ($cm^3 \cdot g^{-1}$)	Average Pore Size (nm)
mb-TiO_2	82.2	0.22	10.5
C-mb-TiO_2	81.8	0.22	10.4
Pd/mb-TiO_2	78	0.20	10.2
Pd/C-mb-TiO_2	79	0.19	10.1

To obtain more information about the surface morphology, the samples were characterized by SEM and HRTEM. Figure S1 shows the SEM images of C-mb-TiO_2, which is fibrous whisker with a uniform width of 300–400 nm, and the morphology shows little change from the mb-TiO_2. The structure of Pd-supported C-mb-TiO_2 was further studied by HRTEM and ED mapping. Well-crystallized TiO_2(B) can be observed in Figure 3a; the nanocrystal with lattice fringes of 0.38 nm is assigned to d_{003} of TiO_2(B) facet, and the lattice fringe spacing of 0.35 nm corresponds to d_{101} of anatase [15], with the majority being the anatase phase. Furthermore, we find that the evident anatase phase is covered by a thin area without crystal lattice fringes (see the two yellow dot lines in Figure 3b), which can be ascribed to the generated amorphous carbon species [21], and is consistent with the results of the Raman analysis. Figure 3c shows that the Pd particles are closed to the carbon and anatase phases, but it is difficult to obtain the accurate positioning of Pd from HRTEM images. The loading of Pd is confirmed by elemental mapping, as shown in Figure 3d. The blue regions represent the presence of

Pd on the surface of TiO_2 in the TEM maps. The relatively low levels of carbon cannot be distinguished due to the external introduction of the carbon source during the testing process. The average particle size of Pd on C-mb-TiO_2 (11.2 nm) is very close to that on mb-TiO_2 (10.5 nm), indicating that the size effect of the Pd particles can be ignored.

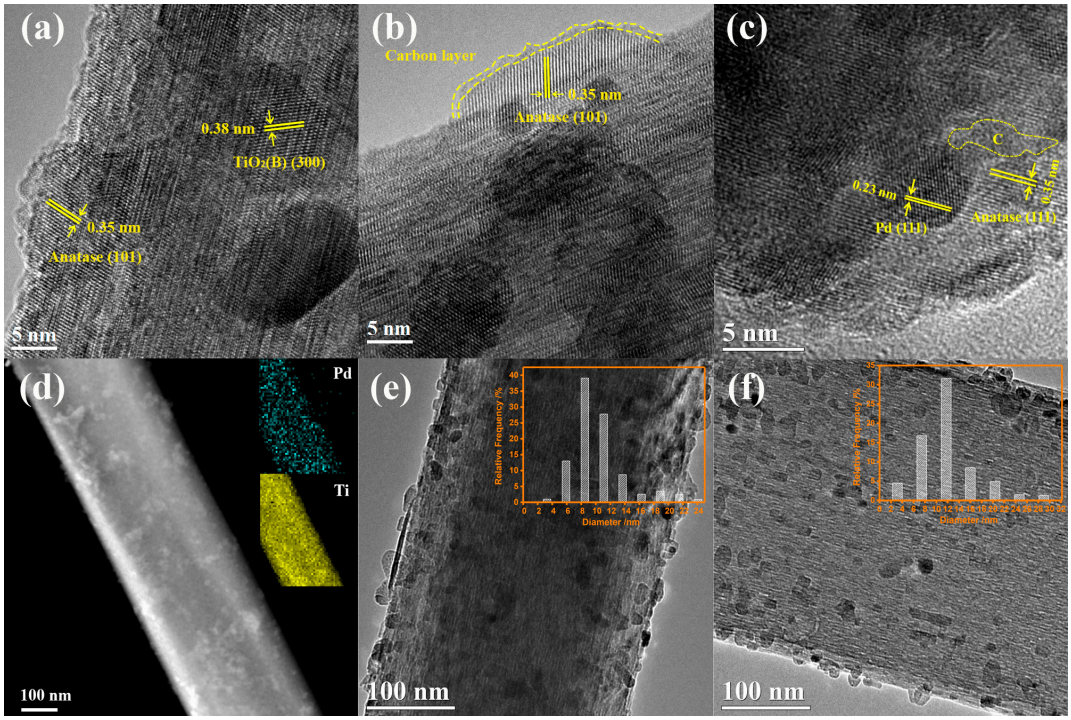

Figure 3. TEM images of the samples: (**a**–**e**) Pd/C-mb-TiO_2 and (**f**) Pd/mb-TiO_2; (**d**) Elemental Pd and Ti maps of Pd/C-mb-TiO_2.

Figure 4 shows the Pd3d core-level spectra of the fresh catalysts. The binding energies at 336.6 and 341.9 eV are ascribed to $Pd^{2+}3d_{5/2}$ and $Pd^{2+}3d_{3/2}$, respectively [23]. The binding energy position of Pd^0 and Pd^{2+} is unchanged between the two catalysts. The presence of Pd^{2+} in the fresh reduced sample is caused by TiO_2-assisted partial oxidation of Pd^0 when exposed to air. As shown in Table S1, the ratio of Pd^{2+}/Pd^0 of the two catalysts is very similar, indicating that the property of active sites is not affected by the carbon heterogeneous modification [11,13]. According to the literature focusing on carbon riveted supported catalysts, the electronic structure of the supported metal would be altered obviously when the generated carbon species are in intimate contact with metallic particles [24,25]. Therefore, it can be deduced that most of the Pd particles deposit onto the TiO_2 phase.

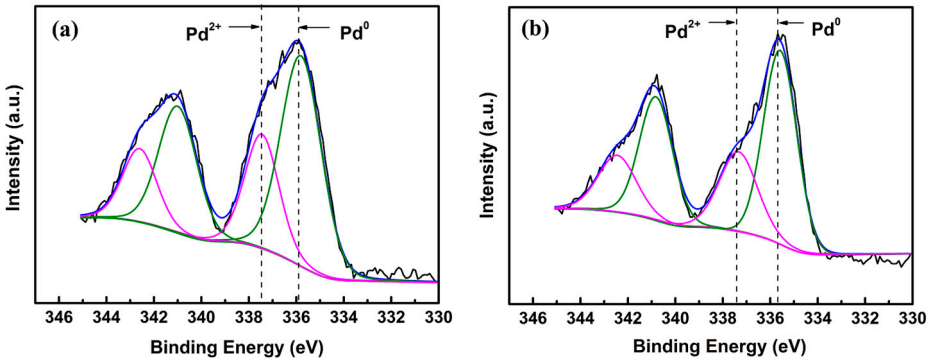

Figure 4. XPS Pd3d spectroscopy of (**a**) Pd/mb-TiO_2 and (**b**) Pd/C-mb-TiO_2.

2.2. The Adsorption Properties of H_2O_2 on the Supports

Isothermal calorimeter was used to investigate the adsorption properties of H_2O_2 on the supports. The adsorption thermodynamic data was calculated from the calorimetric profile recorded through in situ monitoring; the actual amount of adsorbed H_2O_2 was confirmed by the colorimetric method. Finally, their ratio (the adsorption energy of H_2O_2) can be used to represent the interaction strength between H_2O_2 and the support. The detailed process is described in Electronic Supplementary Information (ESI). Figure 5 shows the data of the adsorption properties of H_2O_2 on the support. It can be seen that the adsorption heat of H_2O_2 on C-mb-TiO_2 is obviously lower than that on mb-TiO_2, meaning that the adsorption of H_2O_2 on C-mb-TiO_2 is weaker. The value of adsorption heat of H_2O_2 indicates a reversible physical adsorption. In other words, the generated H_2O_2 is more easily desorbed from the C-mb-TiO_2 surface and H_2O_2 in the reaction medium is more difficult to re-adsorb on the support.

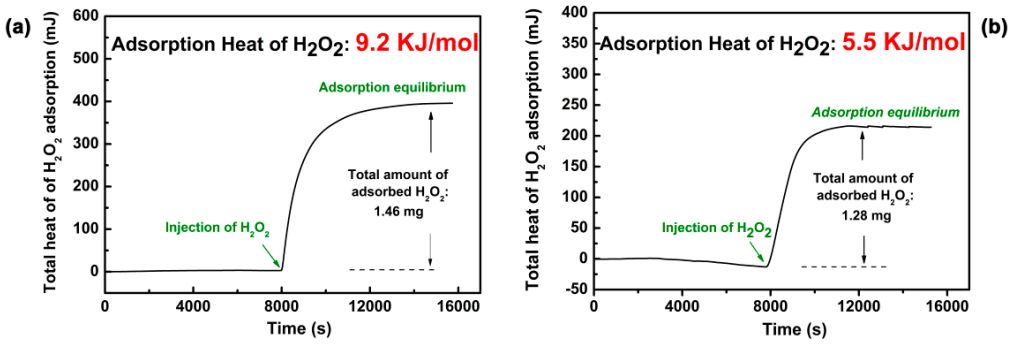

Figure 5. Adsorption heat of H_2O_2 in the studied TiO_2 samples: (**a**) mb-TiO_2 and (**b**) C-mb-TiO_2.

2.3. The Catalytic Activity of the Catalysts

The direct synthesis of H_2O_2 from H_2 and O_2 over Pd/mb-TiO_2 and Pd/C-mb-TiO_2 catalysts were investigated at 283 K and ambient pressure. As shown in Figure 6a, the conversion of H_2 shows little variation over time, while the selectivity and productivity of H_2O_2 decrease along with the time for both catalysts. The Pd/C-mb-TiO_2 catalyst exhibits better activity for H_2O_2 synthesis. The conversion of H_2 over Pd/C-mb-TiO_2 is approximately 35% higher than that over Pd/mb-TiO_2. The Pd/mb-TiO_2 catalyst shows H_2O_2 productivity of 1933 and 1717 mmol/g_{Pd}/h after 0.5 h and 1h, respectively, while the corresponding productivity on Pd/C-mb-TiO_2 is 2848 and 2411 mmol/g_{Pd}/h with an improvement of more than 40%. Meanwhile, the H_2O_2 selectivity over Pd/C-mb-TiO_2 is also promoted by 9% when compared with that over Pd/mb-TiO_2. The analysis above indicates that the catalyst performance is significantly improved due to the carbon modification. Notably, the catalytic performance of both the Pd/mb-TiO_2 and Pd/C-mb-TiO_2 are superior to the Pd/P25 catalyst [4,8,11], which is widely investigated for the direct synthesis of H_2O_2.

To further unveil the effect of the support, we also performed the decomposition and hydrogenation of H_2O_2 under N_2 and N_2/H_2 atmospheres, respectively, which are the two main side reactions in the direct synthesis of H_2O_2. As illustrated in Figure 6b, neither of the catalysts showed activity for the decomposition of H_2O_2 in pure N_2 flow. When the H_2/N_2 mixture was fed into the reactor, the H_2O_2 was catalytically hydrogenated to form H_2O, demonstrating that the hydrogenation of H_2O_2 is mainly responsible for the productivity and selectivity in this system. Similar results have also been observed for Pd/P25 [26]. Furthermore, it is observed that Pd/C-mb-TiO_2 exhibits much lower hydrogenation rate than Pd/mb-TiO_2. Willock et al. suggested that the production of H_2O_2 takes place at the interface between the particle and TiO_2 [27]. Therefore, it is reasonable for us to assume that the properties of both active sites and supports have great impact on the catalytic synthesis of H_2O_2. Additionally, in our previous work, we confirmed that the accelerated desorption of

H_2O_2 from the support can decrease the hydrogenation rate of H_2O_2 and then improve the selectivity towards H_2O_2 over the corresponding catalyst [13]. As mentioned above, the presence of carbon species can significantly weaken the interaction between H_2O_2 and the catalyst under the premise of similar property of active sites. Therefore, it can be concluded that the weaker interaction can reduce the concentration of H_2O_2 on the surface of the catalyst and then decrease the hydrogenation rate of H_2O_2. In addition, the improvement of H_2O_2 desorption can provide more reactive sites for H_2O_2 formation. As a result, the enhanced selectivity of H_2O_2 and the conversion of H_2 improve the productivity of H_2O_2.

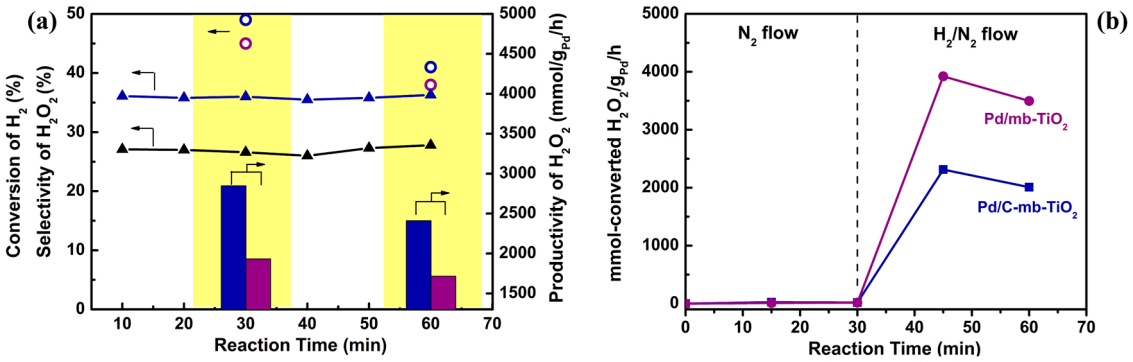

Figure 6. (**a**) H_2 conversion, H_2O_2 selectivity and productivity, and (**b**) decomposition and hydrogenation of H_2O_2 over Pd/mb-TiO_2 and Pd/C-mb-TiO_2. (Blue color indicates Pd/C-mb-TiO_2, purple color indicates Pd/mb-TiO_2. Filled triangles: H_2 conversion. Open circles: H_2O_2 selectivity. Histogram: H_2O_2 productivity).

3. Materials and Methods

3.1. Synthesis of Carbon-Modified TiO_2 Whisker

First, the mesoporous and bicrystalline TiO_2 whisker was prepared according to our previous report [15]. Briefly, $K_2Ti_2O_5$ was suspended in 0.1 M H_2SO_4 solution with vigorous stirring to form $H_2Ti_2O_5$. The suspension was filtered and washed, following which it was dried at 353 K under vacuum and then calcinated at 723 K for 2 h in muffle to obtain mesoporous and bicrystalline TiO_2 whisker. The final catalyst was denoted as mb-TiO_2.

The carbon-modified mb-TiO_2 was prepared as follows [14]. 1 g of mb-TiO_2 was dispersed in 20 mL of dichloromethane containing 0.377 g of benzenephosphonous acid. After stirring for 24 h, the precipitation was filtered and washed with water/acetone (50/50 by volume) solution, and then dried in an oven at 373 K. The dried sample was treated at 673 K in Ar gas flow for 4 h and denoted as C-mb-TiO_2.

3 wt % Pd-supported catalysts were prepared by incipient wetness impregnation. A certain amount of $PdCl_4^{2-}$ solution was slowly dropped into the support under stirring. The paste was left in natural environment for 4 h, following which it was dried at 383 K overnight. Prior to the reaction, all the catalysts were reduced at 573 K in H_2 (40 mL·min^{-1}) for 1 h. For comparison, commercial titania (P25, Degussa Co., Frankfurt am Main, Germany) was loaded with Pd using the same method.

3.2. Catalyst Characterization

X-ray diffraction (XRD) Spectrogram was collected on a D8 Advance X-ray diffractometer operating at a 40 kV with a current of 100 mA with Cu-Kα radiation. The data was collected in the 2θ range from 5° to 60° at a rate of 0.2 s step^{-1}. Raman spectroscopy (Horiba HR 800) with a multichannel air-cooled CCD camera detector was employed to determine the surface crystal phases of supports using a 514.5 nm He-Cd laser beam. Nitrogen adsorption/desorption at −196 °C were achieved by using the TriStarII 3020M machine (Micromeritics Instrument Co., Atlanta, GA, USA). Surface area was

calculated by the BET method; pore volume was determined by N_2 adsorption at a relative pressure of 0.99. The Pd content of the catalysts was confirmed by ICP-AES (PerkinElmer Co., Waltham, MA, USA). SEM for the morphology of catalyst samples was taken by an America Quanta200 environmental scanning electron microscope. The information of dispersion and size of Pd nanoparticles were obtained by high-resolution transmission electron microscopy (HRTEM) performed on a Japan JEM-2100 at 200 kV. XPS was recorded by an AXIS UltraDLD spectrometer with the monochromatic Al Ka X-ray source. The interaction between H_2O_2 and the support was characterized on a TAM air Calorimeter from TA Instruments.

3.3. Catalytic Reaction

The direct synthesis of H_2O_2 was performed under atmosphere pressure in a glass tri-phase reactor. The reagent gases ($H_2/O_2/N_2$ = 9:36:15) with a total flow rate of 60 mL/min were premixed in a steel mixer, and then introduced into the reactor via a frit fixed at the bottom. The temperature of 60 mL slurry containing 50 mg catalyst and 0.38 mL H_2SO_4 was controlled at 10 °C through the water circulated jacket. Vigorous stirring (950 rpm) was adopted to minimize mass transfer resistance. The outlet of the reactor was linked to a gas chromatography equipped with a 5A molecular sieve packed column and a thermal conductivity detector (SP-6890, Rainbow Chemical Instrument Co., Jinan, China), which helped to continuously analyze the conversion of H_2. The concentration of H_2O_2 in the medium was determined by the colorimetric method after the complexation with a $TiOSO_4/H_2SO_4$ reagent using a UV-vis spectrophotometer (UV-2802S, Unico (Shanghai) Instrument Co., Shanghai, China) at a wavelength of 400 nm. The selectivity of H_2O_2 ($S_{H_2O_2}$) was calculated from the following formula:

$$S_{H_2O_2} = \frac{\text{rate of } H_2O_2 \text{ formation } (\text{mol/min})}{\text{rate of } H_2 \text{ conversion } (\text{mol/min})} \times 100\% \quad (1)$$

The reaction of H_2O_2 hydrogenation and decomposition was also implemented. The process was similar to that described above except for the initial composition of reaction medium. H_2O_2 was added to ethanol solution with the concentration of 0.25 wt %, then the decomposition and hydrogenation of H_2O_2 were tested under a flow of pure N_2 (60 mL/min) and a flow of H_2/N_2 (9:51 mL/min), respectively. The same tests using bare supports or the absence of catalysts were also performed under the conditions mentioned above.

4. Conclusions

In this work, a simple heterogeneous carbon modification was applied to introduce carbon species on the surface of mb-TiO_2. Pristine mb-TiO_2 and carbon-modified mb-TiO_2 were used as the supports of Pd-based catalysts for the direct synthesis of H_2O_2. The interaction between H_2O_2 and the supports was characterized by isothermal microcalorimetry. It was demonstrated that the carbon-decorated TiO_2 exhibited weaker interaction with H_2O_2 than that achieved with the pristine TiO_2. Therefore, the carbon-modified catalyst can effectively accelerate the desorption of H_2O_2 from the catalyst surface and reduce the re-adsorption of H_2O_2 in the reaction medium, which benefits the decrease of side reaction and the improvement of H_2O_2 productivity. Meanwhile, the properties of metallic active sites are not influenced by the carbon modification. As a result, the Pd/C-mb-TiO_2 shows better performance for the direct synthesis of H_2O_2 compared with Pd/mb-TiO_2. More than 40% increase in the productivity of H_2O_2 was achieved, and the selectivity of H_2O_2 improved by 9%. In addition, the catalytic performance of both Pd/mb-TiO_2 and Pd/C-mb-TiO_2 are superior to Pd/P25, which is widely investigated for the direct synthesis of H_2O_2. Hence, heterogeneous carbon modification represents a promising approach to tune the properties of the catalysts, as demonstrated here with TiO_2-supported Pd catalyst for H_2O_2 synthesis.

Supplementary Materials: The following are available online at www.mdpi.com/2073-4344/7/6/175/s1, Figure S1: SEM images of (a,b) mb-TiO_2 and (c,d) C-mb-TiO_2, Figure S2: TG and DSC curves of C-mb-TiO_2,

Figure S3: The scheme of reaction process, Table S1: Quantified XPS data for the surface Pd atoms, Table S2: Calorimetric measurement of H_2O_2 adsorption, Table S3: The performance of Pd catalysts for H_2O_2 synthesis, decomposition and hydrogenation.

Acknowledgments: This work was supported by the National Key Basic Research Program of China (2013CB733505, 2013CB733501), the National Natural Science Foundation of China (Nos. 91334202, 21406118), the Natural Science Foundation of Jiangsu Province of China (BK2012421, BK20160993), the Postdoctoral Science Foundation of China (2016M591837), the Research Fund for the Doctoral Program of Higher Education of China (20123221120015), and the Project for Priority Academic Program Development of Jiangsu Higher Education Institutions (PAPD).

Author Contributions: Rui Tu, Jun Li and Xiaohua Lu designed the framework of experiments; Rui Tu and Shuying Chen performed all the experimental work; Rui Tu analyzed the experimental data and wrote the paper; Licheng Li, Suoying Zhang and Jun Li participated in the modification of the article.

Conflicts of Interest: The authors declare no conflict of interest.

References

1. Campos-Martin, J.M.; Blanco-Brieva, G.; Fierro, J.L. Hydrogen peroxide synthesis: An outlook beyond the anthraquinone process. *Angew. Chem. Int. Ed.* **2006**, *45*, 6962–6984. [CrossRef] [PubMed]
2. Landon, P.; Collier, P.J.; Papworth, A.J.; Kiely, C.J.; Hutchings, G.J. Direct formation of hydrogen peroxide from H_2/O_2 using a gold catalyst. *Chem. Commun.* **2002**, *18*, 2058–2059. [CrossRef]
3. Samanta, C. Direct synthesis of hydrogen peroxide from hydrogen and oxygen: An overview of recent developments in the process. *Appl. Catal. A Gen.* **2008**, *350*, 133–149. [CrossRef]
4. Edwards, J.K.; Hutchings, G.J. Palladium and gold-palladium catalysts for the direct synthesis of hydrogen peroxide. *Angew. Chem. Int. Ed.* **2008**, *47*, 9192–9198. [CrossRef] [PubMed]
5. Garcia, T.; Murillo, R.; Agouram, S.; Dejoz, A.; Lazaro, M.J.; Torrente-Murciano, L.; Solsona, B. Highly dispersed encapsulated Au-Pd nanoparticles on ordered mesoporous carbons for the direct synthesis of H_2O_2 from molecular oxygen and hydrogen. *Chem. Commun.* **2012**, *48*, 5316–5318. [CrossRef] [PubMed]
6. Edwards, J.K.; Solsona, B.; Ntainjua, N.E.; Carley, A.F.; Herzing, A.A.; Kiely, C.J.; Hutchings, G.J. Switching off hydrogen peroxide hydrogenation in the direct synthesis process. *Science* **2009**, *323*, 1037–1041. [CrossRef] [PubMed]
7. Yi, Y.; Wang, L.; Li, G.; Guo, H. A review on research progress in the direct synthesis of hydrogen peroxide from hydrogen and oxygen: Noble-metal catalytic method, fuel-cell method and plasma method. *Catal. Sci. Technol.* **2016**, *6*, 1593–1610. [CrossRef]
8. Hu, B.; Deng, W.; Li, R.; Zhang, Q.; Wang, Y.; Delplanque-Janssens, F.; Paul, D.; Desmedt, F.; Miquel, P. Carbon-supported palladium catalysts for the direct synthesis of hydrogen peroxide from hydrogen and oxygen. *J. Catal.* **2014**, *319*, 15–26. [CrossRef]
9. Fu, L.; Chuang, K.T.; Fiedorow, R. Selective oxidation of hydrogen to hydrogen peroxide. *Stud. Surf. Sci. Catal.* **1992**, *72*, 33–41.
10. Ouyang, L.; Da, G.; Tian, P.; Chen, T.; Liang, G.; Xu, J.; Han, Y. Insight into active sites of Pd–Au/TiO_2 catalysts in hydrogen peroxide synthesis directly from H_2 and O_2. *J. Catal.* **2014**, *311*, 129–136. [CrossRef]
11. Ouyang, L.; Tian, P.; Da, G.; Xu, X.; Ao, C.; Chen, T.; Si, R.; Xu, J.; Han, Y. The origin of active sites for direct synthesis of H_2O_2 on Pd/TiO_2 catalysts: Interfaces of Pd and PdO domains. *J. Catal.* **2015**, *321*, 70–80. [CrossRef]
12. Edwards, J.K.; Ntainjua, E.; Carley, A.F.; Herzing, A.A.; Kiely, C.J.; Hutchings, G.J. Direct synthesis of H_2O_2 from H_2 and O_2 over gold, palladium, and gold-palladium catalysts supported on acid-pretreated TiO_2. *Angew. Chem. Int. Ed.* **2009**, *48*, 8512–8515. [CrossRef] [PubMed]
13. Tu, R.; Chen, S.; Cao, W.; Zhang, S.; Li, L.; Ji, T.; Zhu, J.; Li, J.; Lu, X. The effect of H_2O_2 desorption on achieving improved selectivity for direct synthesis of H_2O_2 over TiO_2(B)/anatase supported Pd catalyst. *Catal. Commun.* **2017**, *89*, 69–72. [CrossRef]
14. Li, L.; Zhu, Y.; Lu, X.; Wei, M.; Zhuang, W.; Yang, Z.; Feng, X. Carbon heterogeneous surface modification on a mesoporous TiO_2-supported catalyst and its enhanced hydrodesulfurization performance. *Chem. Commun.* **2012**, *48*, 11525–11527. [CrossRef] [PubMed]
15. Li, W.; Liu, C.; Zhou, Y.; Bai, Y.; Feng, X.; Yang, Z.; Lu, L.; Lu, X.; Chan, K. Enhanced photocatalytic activity in anatase/TiO_2(B) core-shell nanofiber. *J. Phys. Chem. C* **2008**, *112*, 20539–20545. [CrossRef]

16. Li, W.; Bai, Y.; Liu, C.; Yang, Z.; Feng, X.; Lu, X.; van der Laak, N.K.; Chan, K. Highly thermal stable and highly crystalline anatase TiO_2 for photocatalysis. *Environ. Sci. Technol.* **2009**, *43*, 5423–5428. [CrossRef] [PubMed]
17. Bai, Y.; Li, W.; Liu, C.; Yang, Z.; Feng, X.; Lu, X.; Chan, K. Stability of Pt nanoparticles and enhanced photocatalytic performance in mesoporous Pt-(anatase/TiO_2(B)) nanoarchitecture. *J. Mater. Chem.* **2009**, *19*, 7055–7061. [CrossRef]
18. Li, L.; Shi, K.; Tu, R.; Qian, Q.; Li, D.; Yang, Z.; Lu, X. Black TiO_2(B)/anatase bicrystalline TiO_{2-x} nanofibers with enhanced photocatalytic performance. *Chin. J. Catal.* **2015**, *36*, 1943–1948. [CrossRef]
19. Ji, T.; Li, L.; Wang, M.; Yang, Z.; Lu, X. Carbon-protected Au nanoparticles supported on mesoporous TiO_2 for catalytic reduction of p-nitrophenol. *RSC Adv.* **2014**, *4*, 29591–29594. [CrossRef]
20. Huang, J.; Yuan, D.; Zhang, H.; Cao, Y.; Li, G.; Yang, H.; Gao, X. Electrochemical sodium storage of TiO_2(B) nanotubes for sodium ion batteries. *RSC Adv.* **2013**, *3*, 12593–12597. [CrossRef]
21. Chao, K.; Cheng, W.; Yu, T.; Lu, S. Large enhancements in hydrogen production of TiO_2 through a simple carbon decoration. *Carbon* **2013**, *62*, 69–75. [CrossRef]
22. He, Y.; Feng, J.; Du, Y.; Li, D. Controllable synthesis and acetylene hydrogenation performance of supported Pd nanowire and cuboctahedron catalysts. *ACS Catal.* **2012**, *2*, 1703–1710. [CrossRef]
23. Datye, A.K.; Bravo, J.; Nelson, T.R.; Atanasova, P.; Lyubovsky, M.; Pfefferle, L. Catalyst microstructure and methane oxidation reactivity during the Pd↔PdO transformation on alumina supports. *Appl. Catal. A Gen.* **2000**, *198*, 179–196. [CrossRef]
24. Jiang, Z.; Wang, Z.; Chu, Y.; Gu, D.; Yin, G. Ultrahigh stable carbon riveted Pt/TiO_2-C catalyst prepared by in situ carbonized glucose for proton exchange membrane fuel cell. *Energy Environ. Sci.* **2011**, *4*, 728–735. [CrossRef]
25. Song, W.; Chen, Z.; Yang, C.; Yang, Z.; Tai, J.; Nan, Y.; Lu, H. Carbon-coated, methanol-tolerant platinum/graphene catalysts for oxygen reduction reaction with excellent long-term performance. *J. Mater. Chem. A* **2015**, *3*, 1049–1057. [CrossRef]
26. Ao, C.; Tian, P.; Ouyang, L.; Da, G.; Xu, X.; Xu, J.; Han, Y. Dispersing Pd nanoparticles on N-doped TiO_2: A highly selective catalyst for H_2O_2 synthesis. *Catal. Sci. Technol.* **2016**, *6*, 5060–5068. [CrossRef]
27. Thetford, A.; Hutchings, G.J.; Taylor, S.H.; Willock, D.J. The decomposition of H_2O_2 over the components of Au/TiO_2 catalysts. *Proc. R. Soc. A* **2011**, *467*, 1885–1899. [CrossRef]